JOURNAL OF GEOPHYSICAL RESEARCH, VOL. 97, NO. B12, PAGES 17,309–17,315, NOVEMBER 10, 1992

# Magnetic Domain State and Coercivity Predictions for Biogenic Greigite ($Fe_3S_4$): A Comparison of Theory With Magnetosome Observations

JUAN C. DIAZ RICCI AND JOSEPH L. KIRSCHVINK

*Division of Geological and Planetary Sciences, California Institute of Technology, Pasadena*

The discovery of bacteria that precipitate greigite within intracellular organelles (magnetosomes) offers new evidence about the origin of greigite in natural environments. Unlike magnetite, only scarce information is available about the magnetic characteristics of greigite. For this reason, and the present inability to grow these microorganisms in pure culture, it is not known whether or not the magnetosomes in the newly discovered greigite-precipitating bacteria are of single-domain (SD) size, as are the magnetosomes from magnetite-precipitating bacteria. The hypothesis of natural selection for magnetotactic behavior predicts that the greigite-bearing magnetosomes should also be single magnetic domains. Using previously reported magnetic properties and crystallographic features for greigite, we have calculated the size and shape boundaries expected for SD and superparamagnetic (SPM) behavior in this mineral. For further characterization of the greigite crystals, we analyzed the domain state at various length/width ratios assuming crystal shapes of parallelepipeds and prolate spheroids. Magnetite was used as control for the current theories supporting these calculations. We also present a simple algorithm to calculate the upper size limit of single-domain grains. Our results show that the crystals of bacterial greigite characterized so far are located in the region close to the single-domain superparamagnetic boundary and should have relatively low coercivity. If these crystals contribute to the magnetization of sediments, remanence produced by bacterial greigite could be mistaken for large, multidomain magnetite in alternating field demagnetization studies.

## INTRODUCTION

Until recently, the mineral greigite was thought to form naturally by reduction of iron in $H_2S$ rich sedimentary deposits where the low oxygen or redox potentials were the dominant environmental conditions [*Spender et al.*, 1972; *Demitrack*, 1985; *Bazylinski et al.*, 1988; *Bonev et al.*, 1989; *Hilton*, 1990; *Tric et al.*, 1991]. Since *Mann et al.*[1990] and *Rodgers et al.* [1990] reported the discovery of several new types of microorganisms that precipitate greigite-bearing magnetosomes, interest in the magnetic characterization of the bacterial greigite has been renewed because of its implications for paleomagnetism and bacterial evolution.

A related question of importance involves the selection advantage of bacterial magnetotaxis. *Kirschvink and Lowenstam* [1979] first predicted that bacterial magnetites would fall within the single-domain size and shape boundaries calculated by *Butler and Banerjee* [1975]. Natural selection should gradually weed out strains producing small superparamagnetic crystals or larger multidomain particles, both of which would be less efficient at using geomagnetic navigation. All subsequent analyses of $Fe_3O_4$-bearing bacterial magnetosomes with transmission electron microscopy (TEM) have confirmed this prediction (reviewed by *Chang and Kirschvink* [1989]). The discovery of greigite-precipitating magnetotactic bacteria offers the potential to test this hypothesis on yet another ferrimagnetic mineral.

Although literature about greigite is scarce, *Spender et al.* [1972] measured important magnetic parameters of synthetic greigite samples, and these constitute the basis for our attempts to calculate the single-domain stability parameters for various crystal sizes. *Evans and McElhinny* [1969] and *Butler and Banerjee* [1975] have discussed the magnetic properties of small ferromagnetic particles (prolate spheroids and parallelepipeds, respectively), and although a close relationship among size, shape, and coercivity can be observed with both approaches, significant differences reveal a strong dependence on the crystal morphology. Also, while *Evans and McElhinny* [1969] and *Morrish and Yu* [1955] before them did not consider magnetocrystalline anisotropy, *Butler and Banerjee* [1975] developed a more detailed theoretical description of single-domain particles which was based on the calculations of the demagnetizing energies of rectangular blocks done by *Rhodes and Rowlands* [1954] and *Amar* [1958].

Since bacterial greigite (and magnetite) shows certain polymorphism from parallelepiped-like crystals [*Heywood*, 1990] to cubo-octahedral or irregular shapes [*Rodgers et al.*, 1990], we have calculated the stability domain diagram of greigite for both the prolate spheroid and square-cross section parallelepiped shapes. Furthermore, the accompanying amorphous material that was always observed in bacterial [*Mann et al.*, 1990; *Rodgers et al.*, 1990] and synthetic greigite [*Spender et al.*, 1972] makes it difficult to decide whether these crystals are bound by well-formed faces. We therefore tested the measured crystal dimensions against calculations for both shape types. We also used values of shape, size, and coercivity of needle-like grains of greigite reported recently by *Snowball* [1991] for adjusting the diagram to experimental data. The latter was also used as the main criterion to determine whether the coercivity of greigite is dominated by shape or magnetocrystalline anisotropy. Since there is no experimental measurement reported so far about the real value of $K_1$ for greigite, we used the value $10^4$ erg/cm$^3$ which agrees with the high magnetocrystalline anisotropy expected for greigite and fits experimental values of size, shape, and coercivity reported in the literature [*Snowball and Thompson*, 1988; 1990; *Snowball*, 1991]. Although the latter assumption disagrees with the value suggested by *Spender et al.* [1972] ($10^6$ erg/cm$^3$), it describes more accurately the magnetic properties of single-domain grains of greigite found in sediments.

## CALCULATION OF THE SINGLE-DOMAIN TO SUPERPARAMAGNETIC BOUNDARY

The calculation of the threshold size between superparamagnetic (SPM) and single-domain (SD) particles (the SD-SPM boundary, SPB) was carried out according to the approach of *Butler and*



Paper number 92JB01290.
0148-0227/92/92JB-01290$05.00

*Banerjee* [1975]. It has been demonstrated [*Néel*, 1955] that the lower size limit of a stable single-domain can be calculated using the relaxation equation that shows the volume dependence of $\tau$,

$$\tau = f_o^{-1} \cdot e^{\frac{v H_c J_s}{2kT}} \quad (1)$$

where $\tau$ is the relaxation time, $f_0$ is the frequency factor (assumed to be $10^9$ $s^{-1}$), $v$ is the crystal volume, $H_c$ the coercive force, $k$ the Boltzman constant (1.38 x $10^{-16}$ erg °$K^{-1}$), and $J_s$ the saturation magnetization. Assuming that the main contribution to the coercive force comes from shape anisotropy for small grain sizes (<40 nm [*Evans and McElhinny*, 1969]), the coercive force due to shape anisotropy can be calculated by

$$H_c = \Delta N \cdot J_s \quad (2)$$

where $\Delta N$ is the difference between the demagnetization factor along the major ($N_a$) and minor axis ($N_b$).

$$\Delta N = N_b - N_a \quad (3)$$

Since the expressions of $N_a$ and $N_b$ depend on the geometry of the particle, the calculation of $\Delta N$ will depend on whether the particles are prolate spheroids or parallelepipeds. For the prolate spheroids, $N_a$ and $N_b$ were calculated according to the analysis of *Osborn* [1945], whereas for parallelepipeds the evaluation of the demagnetizing factors was based on *Rhodes and Rolands* [1954] and *Amar* [1958] (see Appendix 1). Defining $q$ as the ratio between length and width ($a/b$) of a prismatic grain (or the major/minor axis of a prolate spheroid), the length of a particle can be expressed as a function of $q$. By substituting (2) in (1) and after some rearrangement we obtain the expression

$$SPB = \left(12q^2kT \cdot \frac{1n[\tau f_o]}{\pi J_s^2 \cdot \Delta N}\right)^{1/3} \quad (4)$$

where

$$\Delta N = 2\pi - 6g\,(1, q) \quad (5)$$

We used (4) to estimate the superparamagnetic threshold of prolate spheroids with (3) substituting $\Delta N$ and volume of the grain $v = \pi a^3/6q^2$. For parallelepipeds, the volume of the particle was replaced by $a^3/q^2$ and $\Delta N$ by (5) (typographical errors in the original paper of *Butler and Banerjee* [1975] were corrected) which was derived assuming $2N_b = 4\pi - N_a$ with $N_a(q)$ as shown in Appendix 1, and replacing into (3). The SD-SPM boundary was calculated at $T$ = 290°K, with $\tau$ = 100 s, and $J_s$ equal to 123 emu/cm$^3$ for greigite [*Spender et al.*, 1972] and 480 emu/cm$^3$ for magnetite [*Butler and Banerjee*, 1975].

## CALCULATION OF THE SINGLE-DOMAIN TO TWO-DOMAIN BOUNDARY

For prolate spheroids of greigite, the energetically stable upper size limit for the single-domain to two-domain (SD-2D) transition was calculated by equating the exchange energy involved in a circular spin configuration to the magnetostatic energy of a single-domain grain [*Morrish and Yu*, 1955]. Although this approach ignores magnetocrystalline anisotropy and assumes a circular spin configuration in the SD grains, it estimates adequately the magnetic properties of particles with axial ratios ($q$) less than 7 [*Evans*, 1972]. The expression used was

$$\frac{a^2}{\ln\left[2.38 . 10^7 . \frac{a}{q} - 1\right]} = 24.72 \times 10^{-12} . \frac{q^2}{N_a\,(q)} \quad (6)$$

where $q$ and $a$ are referred to the ratio and major axis, respectively. The demagnetization factor $N_a(q)$ was calculated for various values of $q$ using (17) (see Appendix 1). In Figures 1 and 3 we indicate in solid lines the corresponding lines of SDB for greigite and magnetite at $T$ = 290°K and $\tau$ = 100 s.

The calculation of the SD-2D boundary line for square-cross section parallelepipeds was carried out following the method of *Butler and Banerjee* [1975]. This treatment assumes a negligible contribution of the magnetocrystalline anisotropy on the calculation of the total magnetic energy of a grain (i.e., $2\pi J_s^2/K_1 \geq 10$) and takes into account the magnetostatic energy of fully magnetized domains separated by a single-domain 180° boundary walls. For wall width $\delta$ and the magnetostatic energy of the domain wall $\sigma$, the dependence of the domain wall energy $\sigma$ on the wall width $\delta$ is

$$\sigma = \frac{\sigma_o}{2} \cdot \left[\frac{\delta}{\delta_o} + \frac{\delta_o}{\delta}\right] \quad (7)$$

where $\sigma_o$ and $\delta_o$ are the wall energy and wall width per unit of area of the extended medium [*Amar*, 1958].

If $A$ is the exchange energy constant (in ergs per centimeter) and $K_1$ the first-order magnetocrystalline anisotropy constant (in ergs per cubic centimeter), the energy of a single-domain wall is

$$\sigma_o = 1.83\sqrt{AK_1} \quad (8)$$

For greigite, $K_1$ was assumed to be $10^4$ erg/cm$^3$, compared to the accepted value of 1.3 $10^5$ erg/cm$^3$ for magnetite [*Banerjee and Moskowitz*, 1985]. Estimates of $A$ were made according to *Galt* [1952]. We used $A$ equal to 1.0 x $10^{-6}$ and 1.5 x $10^{-6}$ erg/cm for greigite and magnetite, respectively. The wall energy of greigite per unit of area, $\sigma_o$, is 0.17 erg/cm$^2$. The values of $A$ and $K_1$ for greigite were used further for the calculation of the wall width $\delta_o$ according to *Butler and Banerjee* [1975], where $\delta_o$ was 4.1 x $10^{-5}$ and 1.5 x $10^{-5}$ cm for greigite and magnetite, respectively.

If we define $\eta$ as the fraction of the grain width that corresponds to the wall width ($\delta = \eta . b$) and substitute in (7), the reduced wall energy per unit of volume [*Amar*, 1958] is

$$e_w = q\,\frac{\sigma_o}{4J_s^2} \cdot \left[\frac{\eta}{\delta_o} + \frac{\delta_o\, q^2}{\eta a^2}\right] \quad (9)$$

The reduced magnetostatic energy ($e_m$) of a two-domain grain bearing a single-domain wall was calculated with *Amar's* [1958] $g(p,q)$ function and *Rhodes and Rowlands's* [1954] function $F(p,q)$ (see Appendix 1). Accordingly, $e_m$ for square cross-section parallelepiped grains as function of $\eta$ and $q$ is

$$e_m = q.[(1+\eta).g\left[\frac{1+\eta}{2}, q\right] + (1-\eta).g\left[\frac{1-\eta}{2}, q\right] + \eta.g\left[\frac{\eta}{q}, \frac{1}{q}\right] - \eta \cdot g[\eta,q] - g[1,q]\,] \quad (10)$$

Also, *Rhodes and Rowlands* [1954] have calculated the reduced energy of a fully magnetized parallelepiped $e_{SD}$ by using the function $g(p,q)$ as follows

$$e_{SD} = q \cdot g\,(1,q) \quad (11)$$

Using the expressions of $e_w$, $e_m$, and $e_{SD}$ as functions of $\eta$, $q$, and $a$, we have determined the minimum reduced energy at various $a/b$ ratios of SD grains of greigite and magnetite by calculating the point at which $e_m + e_w$ equals to $e_{SD}$. When $e_m + e_w > e_{SD}$, the SD configuration is stable, and when $e_m + e_w < e_{SD}$, the two-domain configuration of the grain prevails.

*Bulter and Banerjee* [1975] have proposed a scheme for the calculation of the SDB which consists in the successive evaluation of the minima values of the total energy associated with the particles of different widths, and equating with the energy of an identical fully magnetized grain. The resulting particle size gives the critical particle size attainable before becoming a two-domain grain. Although this method provides a reliable procedure for the calculation of the

SD-2D boundary, it is extremely tedious. For this reason we propose an alternative method which is much easier, faster, and entirely consistent with the *Butler and Banerjee* [1975] proposal.

The changes we suggest consist in a simple mathematical strategy that evaluates the length of the particle under a double constraint, namely, at the minimum value of the total reduced energy of a two-domain grain $e = e_m + e_w$ and at the value of $q$ that makes

$$e_{SD} = e_m + e_w \qquad (12)$$

As the length of the particle ($a$) is a variable only in the expression of $e_w$ (equation (9)), it allows us to calculate the minimum particle sizes attainable for different wall widths (evaluated through $\eta$) at the values of $q$ that satisfy (12). The latter condition is met by evaluating the minima of the partial derivative of (13) respect to $\eta$, at $q$ constant

$$a = \left(\frac{\sigma_o \delta_o^2 q^3}{4\eta\delta_o J_s^2 \cdot (e_{SD}-e_m) - q\sigma_o\eta^2}\right)^{1/2} \qquad (13)$$

After some mathematical manipulations we come up with (14) which is ultimately only a function of $\eta$ and $q$.

$$4q\delta_o J_s^2 \cdot g(1,q) = 2\eta q\sigma_o + 4\delta_o J_s^2\eta \cdot dem(\eta, q) + 4\delta_o J_s^2 \cdot e_m(\eta, q) \qquad (14)$$

where

$$dem(\eta,q) = \left[\frac{\partial e_m(\eta,q)}{\partial \eta}\right]_q \qquad (15)$$

From (14) we calculate the wall widths when the minimum length is established for various $q$, and the minima lengths are recalculated with (13) using the corresponding values of $\eta$ and $q$. Further details of this calculation are given in Appendix 2.

## Calculation of the Coercivities for Different Grain Size

The calculation of the bulk coercivity ($H_B$) of particles of greigite of different sizes was conducted according to *Evans and McElhinny*

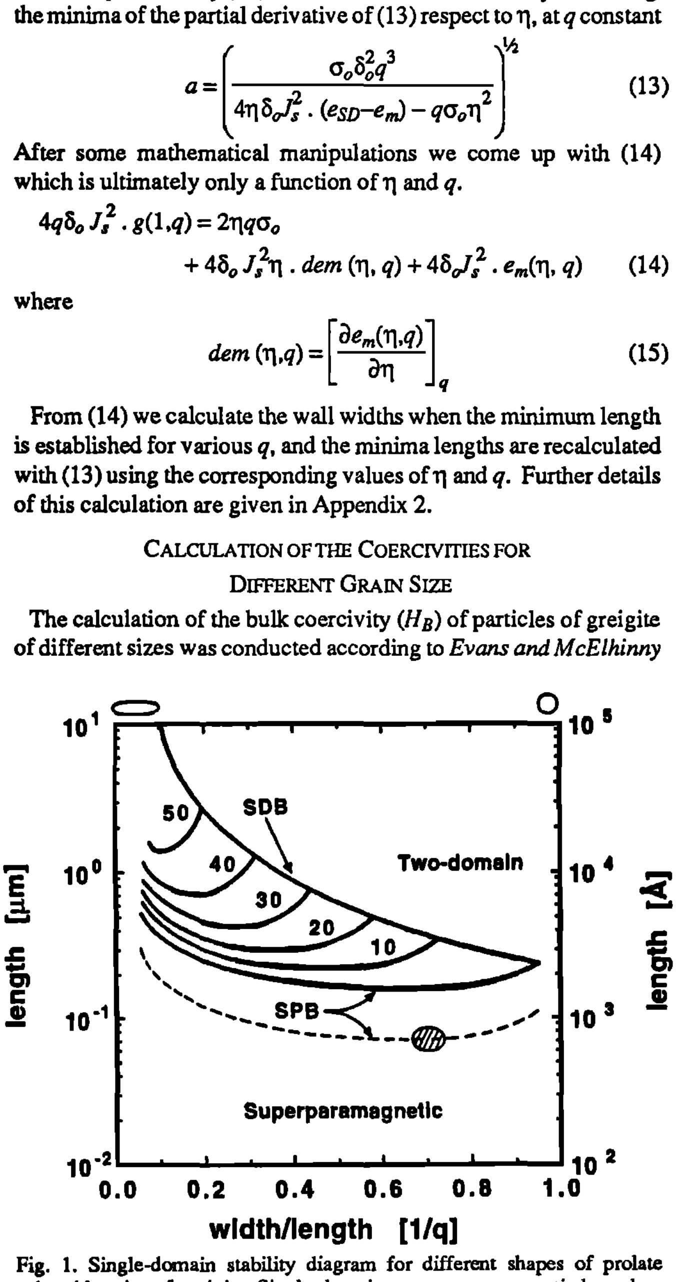


Fig. 1. Single-domain stability diagram for different shapes of prolate spheroid grains of greigite. Single-domain to superparamagnetic boundary (SPB, solid line) and single-domain to two-domain boundary (SDB) were calculated using $J_s$ = 123 emu/cm$^3$, $\tau$ = 100 s, and $T$ = 290°K. Coercivities ($H_b$) are expressed in milliteslas. The shaded oval represents the location of a single-domain crystal of greigite assuming a minor/major axis ratio ($1/q$) equal to 0.70 and length $a$ = 0.07 µm [*Heywood et al.*, 1990]. Neglecting the magnetocrystalline anisotropy, for a spheric grain ($1/q$ = 1), $d_o$ is 0.23 µm. The dashed line represents the SPB calculated at 290°K and for a relaxation factor $\tau = 10^{-8}$ s.

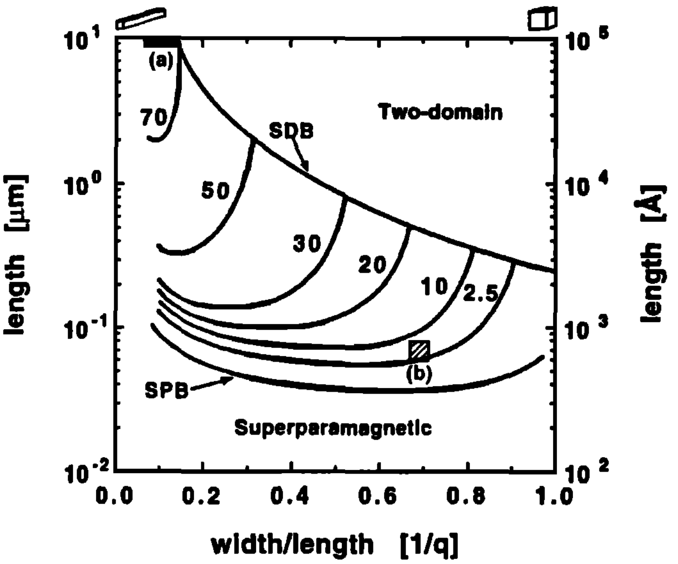


Fig. 2. Single-domain stability diagram for greigite prisms. Single-domain to superparamagnetic boundary (SPB) and single- to two-domain boundary (SDB) were calculated using $J_s$ = 123 emu/cm$^3$, $\tau$ = 100 s, $T$ = 290°K, $\sigma_o$ = 0.17 erg/cm$^2$, and $\delta_o$ = 4.1 $10^{-5}$ cm. Coercivities ($H_b$) are expressed in milliteslas. The rectangle a represents the location of needle-like single domain crystals of greigite that show axial ratios 0.05 < ($1/q$) < 0.1, length > 10 µm, and coercivities $H_b$ = 60 mT [*Snowball*, 1991]. The square b represents the location of a single-domain crystal of greigite assuming an axial ratio ($1/q$) equal to 0.70, length $a$ = 0.07 µm [*Heywood et al.*, 1990], and bulk coercivity $H_b$ = 4 mT (for further details, see Figure 5). Assuming values of $\sigma_o$ and $\delta_o$ as mentioned above, for a cubic grain, $d_o$ is 0.25 µm.

[1969]. Equation (16) was evaluated for different values of $a$ and $q$, and the expression of volume ($v$) was also changed depending on whether the grain under consideration was a prolate spheroid ($\pi a^3/6q^2$) or a square cross-section parallelepiped ($a^3/q^2$).

$$H_B = H_c - \left(\frac{2kTH_c(Q + \ln\tau)}{J_s v}\right)^{1/2} \qquad (16)$$

where $H_B$ is the coercivity required to unblock the magnetic dipole of a grain, $H_c$ is the theoretical or microscopic coercivity, and $Q$ a numerical value equal to 22 [*Evans and McElhinny*, 1969]. Also, the values used for $H_c$ were calculated according to (2) and (3) taking into account the shape of the grains.

## Results

Figures 1 and 2 show the stability diagrams of single-domain crystals of greigite for prolate spheroids and rectangular parallelepipeds, respectively. Within the diagrams we have located the position of biogenic greigite crystals, reported by *Heywood et al.* [1990]. Figure 1 shows that, if the bacterial greigite grains are prolate spheroids, they would be superparamagnetic and would not have a magnetic moment locked in any particular orientation. The superparamagnetic grains would have relaxation times ($\tau$) of the order of nanoseconds (Figure 1). However, if the same bacterial greigite grain were prismatic in shape, Figure 2 implies that they would fall into the SD region with an estimated bulk coercivity of 4 mT, though close to the SD-SPM boundary. Also, we have included in the diagram presented in Figure 2, the location of SD needle-like grains of greigite (~10 µm long) that showed coercivities higher than 50 mT reported by *Snowball* [1991].

Because we used an iterative computational method for calculating all the lines presented in Figures 1 and 2, we tested the algorithms for magnetite, comparing to previous calculations as a control. In Figures 3 and 4 we present our results for prolate spheroids and

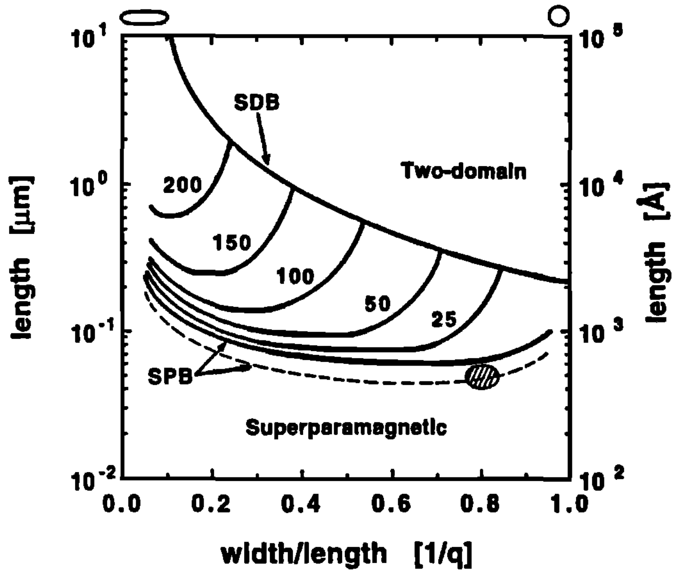


Fig. 3. Single-domain stability diagram for different shapes of prolate spheroid grains of magnetite. SD-SPM boundary (SPB) and SD-2D boundary (SDB) were calculated using $J_s$ = 480 emu/cm$^3$, $\tau$ = 100 s, and $T$ = 290°K. Coercivities ($H_b$) are expressed in milliteslas. The shaded oval represents the location of a single-domain crystal of magnetite assuming a minor/major axis ratio ($1/q$) equal to 0.8 and length $a$ = 0.05 µm [*Mann et al.*, 1987*b*]. Neglecting the magnetocrystalline anisotropy and for a spheric grain ($1/q$ = 1), $d_o$ is 0.21 µm. The dashed line represents the SPB line that contains the grain of magnetite and corresponds to either $T$ = 290°K and $\tau = 10^4$ s or $T$ = 120°K and $\tau$ = 100 s.

square cross-section parallelepipeds of magnetite respectively. In both cases, the curves agree fairly well with previous reports [*Evans and McElhinny*, 1969; *Butler and Banerjee*, 1975], indicating that the algorithms were executed satisfactorily. However, as we were not able to find any previous calculation of the contours of constant coercivity for magnetite parallelepipeds in the literature, we felt it worthwhile to include them on Figure 4 here. Note that the SD field for the prolate spheroids (Figure 3) occurs at larger crystal dimensions than for the parallelepipeds (Figure 4). It could be explained simply because a parallelepiped has nearly twice ($6/\pi$) the volume of a square spheroid of the same dimensions, or by the effect of the magnetic circular spin configuration assumed in this model. If a magnetic circular spin array takes place, it will contribute to a higher stabilization of the SD grain, so a larger crystal would be needed to develop a boundary wall. However, a circular spin structure is energetically unfavorable in greigite and magnetite because of their high magnetocrystalline anisotropies [*McElhinny*, 1979].

From Figures 1-4 we conclude that the magnetic characteristics of SD particles of biogenic greigite and magnetite are more consistent with prismatic rather than ellipsoidal particles. We have accordingly estimated the maximum size of a cubic SD particle ($d_o$) and have calculated the bulk coercivity ($H_b$) of bacterial greigite assuming that they are indeed square cross-section parallelepipeds. From Figures 2 and 4 we estimate the maximum SD size of a cubic grain at the SD-2D boundary ($d_o$) to be 0.25 and 0.082 µm for greigite and magnetite respectively. While we have no previous estimates of $d_o$ for greigite for comparison, the value of $d_o$ for magnetite agrees fairly well with previous reports [*Worm et al.*, 1991] that suggest 0.076 µm [*Butler and Banerjee*, 1975] and 0.096 µm [*Wyn and Dunlop*, 1989]. The values of $d_o$ estimated when the particles were considered prolate ellipsoids are 0.23 µm and 0.21 µm for greigite and magnetite, respectively (Figures 1 and 3).

In Figure 5 we show in greater detail the lower-right hand corner of Figure 2, with the locations of crystals of greigite reported by *Rodgers et al.* [1990] and *Heywood et al.* [1990]. The crystals fall

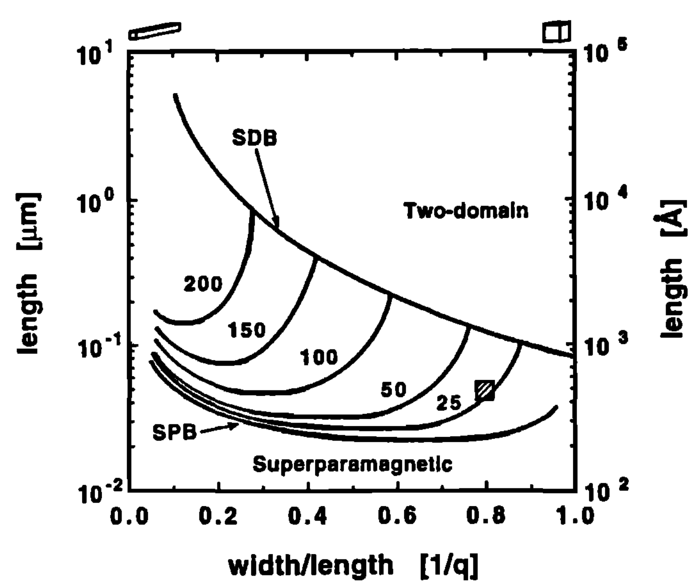


Fig. 4. Single-domain stability diagram for magnetite prisms. SD-SPM boundary (SPB) and SD-2D boundary (SDB) were calculated using $J_s$ = 480 emu/cm$^3$, $\tau$ = 100 s, $T$ = 290°K, $\sigma_o$ = 0.8 erg/cm$^2$, and $\delta_o$ = 1.5 10$^{-5}$ cm. Coercivities ($H_b$) are expressed in milliteslas. The square represents the location of an average single domain crystal of magnetite assuming an axial ratio ($1/q$) equal to 0.8, length $a$ = 0.05 µm [*Mann et al.*, 1987*b*], and bulk coercivity $H_b$ = 30 mT [*Mann et al.*, 1987*a*]. Assuming values of $\sigma_o$ and $\delta_o$ as mentioned above, for a cubic grain, $d_o$ is 0.082 µm.

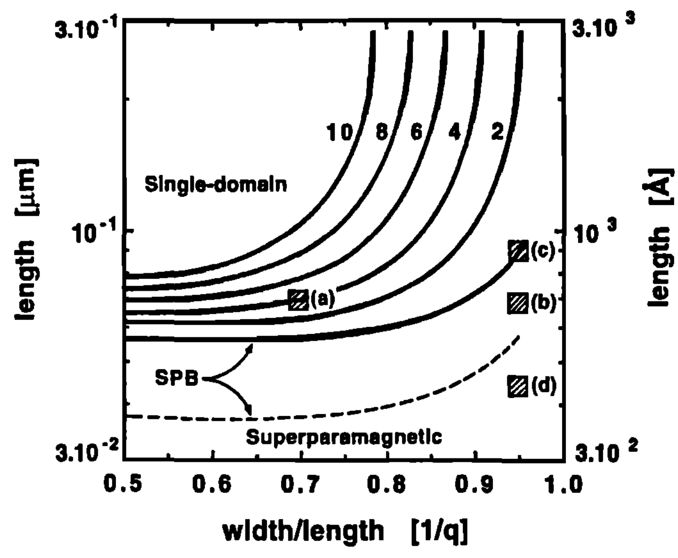


Fig. 5. Detailed single-domain stability diagram of greigite parallelepipeds. Coercivities ($H_b$) from 10 to 2 milliteslas were calculated for various shapes and sizes of greigite grains. Single-domain to superparamagnetic boundary (SPB) lines were calculated using $J_s$ = 123 emu/cm$^3$, $\tau$ = 100 s, $\sigma_o$ = 0.17 erg/cm$^2$, and $\delta_o$ = 4.1 10$^{-5}$ cm, and $T$ = 290°K (solid line) and $T$ = 77°K (dashed line). Square a represents the location of a well-defined grains of greigite with axial ratio ($1/q$) equal to 0.70 and length $a$ = 0.07 µm [*Heywood et al.*, 1990]. The bulk coercivity corresponding to the grain (square a) is $H_b$ = 4 mT. Square b depicts a well-defined cuboidal crystal found in other type of bacteria with $1/q$ = 0.95 and $a$ = 0.067 µm [*Heywood et al.*, 1990]. Square c represents the location of a less well defined grain of greigite observed within magnetosomes of other bacteria with axial ratio about $1/q$ = 0.95 and length $a$ = 0.09 µm (includes the crystalline plus the amorphous material) [*Rodgers et al.*, 1990]. Square d depicts the location of only the crystalline structure observed in the latter greigite magnetosomes, with $1/q$ = 0.95 and $a$ = 0.045 µm [*Rodgers et al.*, 1990].

in two different regions depending on the shape of the grains. The cuboidal crystals (we assumed $1/q = 0.95$ for better illustration) fall in the superparamagnetic field (square b), whereas the more elongate particles are in the region of single-domain particles (square a). For cuboidal grains located on the SD-SPM boundary, measurements of coercivity would fail at room temperature (290°-300°K), whereas measurements of the coercivity would be possible at the lower temperatures used by *Spender et al.* [1972] as a consequence of the downward shift of the SD-SPM transition. Figure 5 also shows the location of the less defined greigite crystal observed by *Rodgers et al.* [1990] in the "many-celled prokaryote" (square d in Figure 5). This "mulberry-like prokaryote" presents magnetosomes loaded with crystalline (~45 nm) and amorphous phases (20 nm width), both identified as greigite. While the whole magnetosome (crystalline plus amorphous phases, 85-90 nm) could be located close to the SD region (square c) (assuming $1/q = 0.95$), the crystalline structure (square d) that would truly contribute to the magnetic coercivity falls below the SPB calculated at 77°K (Figure 5). For the latter (square d), measurements of coercivity would need temperatures below 50°K.

In Figure 6 we show the influence of the shape and size of greigite and magnetite grains on the width ($\eta$) of the single-domain 180° boundary walls. Although the values of $J_s$ and $K_1$ for greigite and magnetite are significantly different, the widths of the walls show identical behavior for different size and shape of the grains. For values of $\sigma_0$ and $\delta_0$ corresponding to higher $K_1$ the wall boundary width decreases (results not shown). We also show in Figure 6 that for greigite and magnetite the largest boundary wall is developed in cubic particles with a maximum width of 55-57% of the grain width.

As we mentioned above, we have used estimates of the exchange energy ($A$) and magnetocrystalline anisotropy ($K_1$) constants for the calculation of $\sigma_0$ and $\delta_0$ (equations (7) and (8)) because of the lack of any experimental values. For this reason we used the routine described here to study the influence of $\delta_0$ and $\sigma_0$ on the position of SD-2D boundary line with the aim to see how sensitive the boundary is to these parameters. In Figure 7 we present the effect of varying $\sigma_0$ on this boundary and in Figure 8 the influence of various values of $\delta_0$ on it. From both figures we see that the influence of $\sigma_0$ and $\delta_0$ is exerted only for larger crystals of greigite, which would correspond at least to cubic particles larger that 0.13 μm (see Figure 8 for $\delta_0 = 0.5 \times 10^{-5}$ cm). From Figures 7 and 8 we can also see that the change of both parameters is not enough to modify our previous observations.

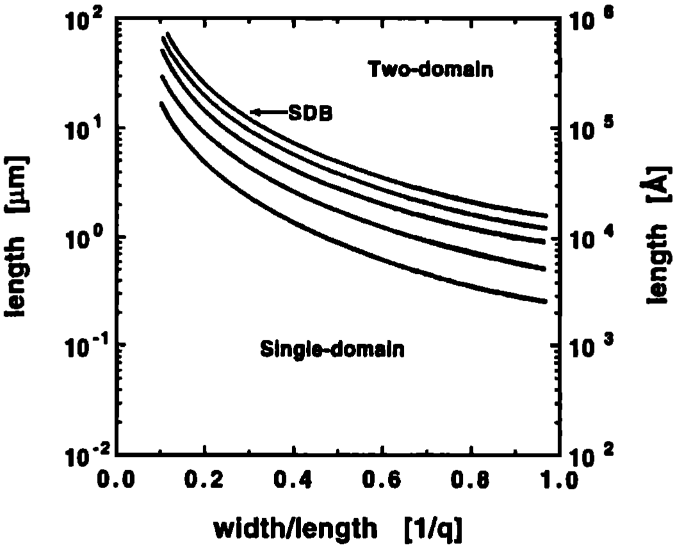


Fig. 7. Single-domain to two-domain boundary (SDB) of prismatic greigite grains as function of the axial ratio (width/length) and for different values of the wall energy $\sigma_0$. For the calculation we used the parameter values indicated in Figure 2, $\delta_0 = 4.1 \, 10^{-5}$ cm, and $\sigma_0$ equal to 0.17, 0.5, 1.0, 1.5, and 2.0 from lower to upper line, respectively.

## DISCUSSION

Although the influence of the shape of the particles (prolate spheroids or square-cross section prisms) is relatively small for magnetite (Figures 3 and 4), it affects significantly the stability diagram of greigite regardless the particular values of $\delta_0$ or $\sigma_0$. Hence the surface morphology of a greigite crystal is important, since the magnetic properties change a great amount. Also, Figures 1 and 3 show that the circular spin configuration assumed for calculating the

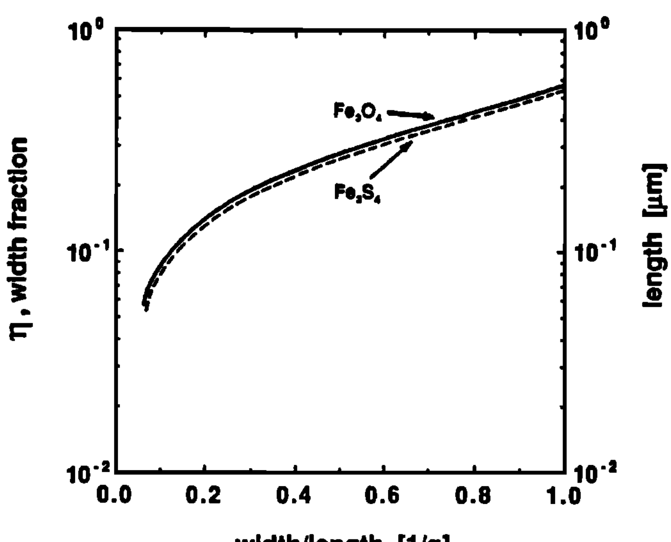


Fig. 6. Width ratio of the 180° boundary wall ($\eta$ = wall width/grain width) and length of different grains of greigite ($Fe_3S_4$) and magnetite ($Fe_3O_4$) as a function of the shape (width/length).

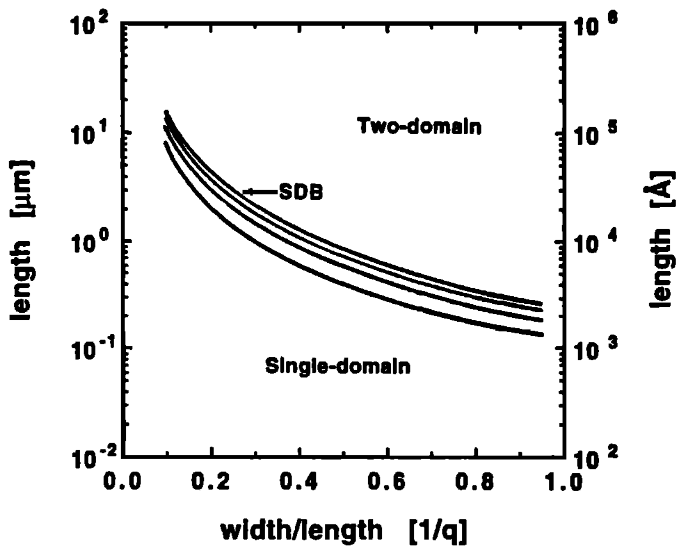


Fig. 8. Single-domain to two-domain boundary (SDB) of prismatic greigite grains as function of the axial ratio (width/length) and for different values of the wall width of the extended medium $\delta_0$. For the calculation we used the parameter values indicated in Figure 2, $\sigma_0 = 0.17$ erg/cm$^2$, and $\delta_0$ equal to 0.5, 1.0, 2.0, and 4.0 $10^{-5}$ cm from lower to upper line, respectively.

SD-2D boundary in prolate spheroids [*Morrish and Yu*, 1955] is inappropriate for these materials that have very high values of magnetocrystalline anisotropy ($K_1$) [*McElhinny*, 1979]. Although *Moon and Merrill* [1988] have applied a more accurate approach for the calculation of the total reduced magnetic energy for a prolate spheroid without the incorporation of a circular spin configuration, we concluded that the bulk coercivity of bacterial greigite could be better estimated if we assume the particles are parallelepipeds. We have estimated a $H_b = 4.0 \pm 0.5$ mT for the longer particles, whereas the rounded or cubic grains fell into the superparamagnetic region close to the SD-SPM boundary showing a relaxation time $\tau \approx 10^{-3}$ s.

The high value of $K_1$ of greigite assumed by *Spender* [1972] of $10^6$ erg/cm$^3$ is incompatible with more recent experimental data of $H_b$ of greigite. If $K_1$ were of the order of $10^6$, the values of $\delta_o$, $\sigma_o$, coercivity, and SD-SPM boundaries would all be different. The changes would suggest that the phenomenon of magnetization will be totally dominated by magnetocrystalline anisotropy ($2\pi J_s^2/K_1 \sim 0.1$) and the formation of two-domain particles will be a highly unfavorable process even for very large crystals. Furthermore, it would be possible to observe at room temperature SD particles as small as 10 nm; this is rather unlikely and in fact contradicts the observation of *Uda* [1968] when he was unable to determine the coercivity of synthetic grains of greigite with sizes ranging from 30 to 50 nm. Although the degree of uncertainty incorporated by the assumption of $K_1$ and the estimates of $\sigma_o$ and $\delta_o$ will modify the values of $d_o$ and the precise location of the SD-2D line (SDB), it will not alter our conclusions concerning the location of bacterial greigite grains within the lower part of the magnetic domain diagram.

Our results allow us to explain the unsuccessful attempts to measure the coercivity of synthetic greigite [*Uda*, 1968], the increasing of coercivities at lower temperatures [*Spender et al.*, 1972] and the lower remanent magnetization observed in bacterial enrichments [*Mann et al.*, 1990, *Rodgers et al.*, 1990] that did not form a packed pellet close to a magnetic bar, as it is usually observed in other strongly magnetic organisms (magnetite-precipitating bacteria) [*Blakemore*, 1975; *Moench and Konetzka*, 1978].

The slight discrepancy between our result of $d_o$ (0.082 μm) for magnetite and the value reported by *Butler and Banerjee* [1975] (0.076 μm) is not easy to explain because the routine we used is based largely on their analysis. Our procedure, however, does not involve a graphical minimization, and this may explain this minor difference.

Finally, for paleomagnetic studies our results suggest that alternating field demagnetization may be one of the simplest ways of removing a greigite magnetic component from a sample with several magnetic minerals present.

## APPENDIX 1

The expressions used for the calculation of demagnetizing factor of prolate spheroids were obtained from *Osborn* [1945].

$$Na(q) = \frac{1}{1-q^2}\left[1 - \left[\frac{q}{2\sqrt{q^2-1}}\ln\frac{q+\sqrt{q^2-1}}{q-\sqrt{q^2-1}}\right]\right] \tag{17}$$

$$Nb(q) = \frac{q}{2(q^2-1)}\left[q - \left[\frac{1}{2\sqrt{q^2-1}}\ln\frac{q+\sqrt{q^2-1}}{q-\sqrt{q^2-1}}\right]\right] \tag{18}$$

The demagnetizing factors of parallelepipeds were calculated according to *Butler and Banerjee* [1975],

$$Na(q) = 4 \cdot g(1,q) \tag{19}$$

where, from *Amar* [1958],

$$g(p,q) = \frac{F(p,0) - F(p,q)}{pq} \tag{20}$$

and, from *Rhodes and Rowlands* [1954],

$$\begin{aligned} F(p,q) = {} & (p^2-q^2)\sinh^{-1}\left[\frac{1}{\sqrt{p^2+q^2}}\right] + p(1-q^2)\sinh^{-1}\left[\frac{p}{\sqrt{1+q^2}}\right] \\ & + pq^2\sinh^{-1}\left[\frac{p}{q}\right] + q^2\sinh^{-1}\left[\frac{1}{q}\right] + 2pq\tan^{-1}\left[\left(\frac{q}{p}\right)\sqrt{1+p^2+q^2}\right] \\ & - \left(\frac{1}{3}\right)(1+p^2-2q^2)\sqrt{1+p^2+q^2} + \left(\frac{1}{3}\right)(1-2q^2)\sqrt{1+q^2} \\ & + \left(\frac{1}{3}\right)(p^2-2q^2)\sqrt{p^2+q^2} - \pi pq + \left(\frac{2}{3}\right)q^3 \end{aligned} \tag{21}$$

## APPENDIX 2

The expression of the total reduced energy of a grain $e_m + e_w$ satisfying one of the boundary conditions can be written as

$$F(\eta,q,a) = e_m(\eta,q) + e_w(\eta,q,a) - e_{SD}(q) = 0 \tag{22}$$

and according to (13), $a$ can be written as

$$a = G(\eta,q) \tag{23}$$

Therefore, applying the second boundary condition, we get

$$\left[\frac{\partial a}{\partial \eta}\right]_q = \left[\frac{\partial G(\eta,q)}{\partial \eta}\right]_q = 0 \tag{24}$$

After some manipulation we obtained (14) mentioned above, where

$$\begin{aligned} \left[\frac{\partial e_m(\eta,q)}{\partial \eta}\right]_q = {} & q \cdot [g\left[\frac{\eta}{q},\frac{1}{q}\right] + \eta \cdot E - g\left[\frac{1-\eta}{2},q\right] + (1-\eta) \cdot D \\ & + g\left[\frac{1+\eta}{2},q\right] + (1+\eta) \cdot C - g(\eta,q) - \eta \cdot B\,] \end{aligned} \tag{25}$$

and

$$B = \left[\frac{\partial g(\eta,q)}{\partial \eta}\right]_q \tag{26}$$

$$C = \left[\frac{\partial g\left(\frac{1+\eta}{2},q\right)}{\partial \eta}\right]_q \tag{27}$$

$$D = \left[\frac{\partial g\left(\frac{1-\eta}{2},q\right)}{\partial \eta}\right]_q \tag{28}$$

$$E = \left[\frac{\partial g\left(\frac{\eta}{q},\frac{1}{q}\right)}{\partial \eta}\right]_q \tag{29}$$

The evaluation of the coefficients $B$ - $E$ implies the evaluation of (30) for $p$ and $q$ taking the corresponding expression shown in (26)-(29).

$$\left[\frac{\partial F(p,q)}{\partial \eta}\right]_q \tag{30}$$

Because the derivations for the coefficients $B$ - $E$ are too cumbersome, they are not presented here. These derivations, as well as IBM-based MATHCAD$^R$ routines, are available upon request.

*Acknowledgments.* This work was supported partially by NIH grant GM41635 and is contribution 5043 from the Division of Geological and Planetary Sciences of the California Institute of Technology.

## REFERENCES


Amar, H., Size dependence of the wall characteristics in a two-domain iron particle, *J. Appl. Phys.*, *29*, 542-543, 1958.

Banerjee, S. K., and B. M. Moskowitz, Ferrimagnetic properties of magnetite, in *Magnetite Biomineralization and Magnetoreception in Organisms*, edited by J. L. Kirschvink, *et al.*, pp. 17-41, Plenum, N.Y., 1985.

Bazylinski, D. A., R. B. Frankel, and H. W. Jannasch, Anaerobic magnetite production by a marine, magnetotactic bacterium, *Nature, 334*, 518-519, 1988.

Blakemore, R. P., Magnetotactic bacteria, *Science, 190*, 377-379, 1975.

Bonev, I. K., K. G. Khrischev, H. N. Neokov, and V. M. Gerogiev. Mackinanite and greigite in iron sulfide concretions from Black-sea sediments, *Dok. Bolg. Akad. Nauk.*, *42*, 97-100, 1989.

Butler, R. F., and S. K. Banerjee, Theoretical single-domain grain size range in magnetite and titanomagnetit, *J. Geophys. Res.*, *80*, 4049-4058, 1975.

Chang, S. R., and J. L. Kirschvink, Magnetofossils, the magnetization of sediments,and the evolution of magnetite biomineralization, *Annu. Rev. Earth Planet. Sci.*, *17*, 169-195, 1989.

Demitrack, A., A search for bacterial magnetite in the sediments of Eal Marsh,Woods Hole, Massachusetts, in *Magnetite Biomineralization and Magnetoreception in Organisms*, edited by Kirschvink *et al.*, pp. 625-645, Plenum, N.Y., 1985.

Evans, M. E., Single-domain particles and TRM in rocks, *Commun. Earth. Sci. Geophys.*, *2*, 139-148, 1972.

Evans, M. E., and M. W. McElhinny, An investigation of the origin of stable remanence in magnetite-bearing igneous rocks, *J. Geomag. Geoelect.*, *21*, 757-773, 1969.

Galt, J. K., Motion of a ferromagnetic domain wall in $Fe_3O_4$, *Phys. Rev.*, *85*, 664-669, 1952.

Heywood, B. R., D. A. Bazylinski, A. Garratt-Reed, S. Mann, and R. B. Frankel, Controlled biosynthesis of greigite ($Fe_3O_4$) in magnetotactic bacteria, *Naturwissen*, *77*, 536-538, 1990.

Hilton, J., Greigite and the magnetic properties of sediments, *Limnol. Oceanogr.*, *35*, 509-520, 1990.

Kirschvink, J. L. and H. A. Lowenstam, Mineralization and magnetization of chiton teeth: Paleomagnetic, sedimentologic, and biologic implications of organic magnetite, *Earth and Planet. Sci. Lett.*, *44*, 193-204, 1979.

Mann, S., N. H. C. Sparks, and R. P. Blakemore, Ultrastructure and characterization of anisotropic magnetic inclusions in magnetotactic bacteria, *Proc. R. Soc. London B, Ser. F*, *231*, 469-476, 1987*a*.

Mann, S., N. H. C. Sparks, and R. P. Blakemore, Structure, morphology and crystal growth of anisotropic magnetite crystals in magnetotactic bacteria, *Proc. R. Soc. London B, Ser. F*, *231*, 477-487, 1987*b*.

Mann, S., N. H. C. Sparks, R. B. Frankel, D. A. Bazylinski, and H. W. Jannasch, Controlled biosynthesis of greigite ($Fe_3O_4$) in magnetotactic bacteria, *Nature*, *343*, 258-261, 1990.

McElhinny, M. W., Rock magnetism, in *Palaeomagnetism and plate tectonics* edited by W. B. Harland *et al.*, p.32-67, Cambridge University Press, New York, 1979.

Moench, T. T., and W.A. Konetzka, A novel method for the isolation and study of a magnetostatic bacterium, *Arch. Microbiol.*, *119*, 203-212, 1978.

Moon, Th. and R. L. Merrill, Single-domain theory of remanent magnetization, *J. Geophys. Res.*, *93*, 9202-9210, 1988.

Morrish, A. H., and S. P. Yu, Dependence of the coercive force on the density of some iron oxide powders, *J. Appl. Phys.*, *26*, 1049-1055, 1955.

Néel, L., Some theoretical aspects of rock-magnetism, *Advan.Phys.*, *4*, 191-243, 1955.

Osborn, J. A., Demagnetizing factors of the general ellipsoid, *Phys.Rev.*, *67*, 351-357, 1945.

Rhodes, P., and G. Rowlands, Demagnetising energies of uniformly magnetised rectangular blocks, *Proc. Leeds Philos. Lit. Soc., Sci. Sect.*, *6*, 191-210, 1954.

Rodgers, F. G., R. P. Blakemore, N.A. Blakemore, R. B. Frankel, D. A. Bazylinski, D. Maratea, and C. Rodgers, Intracellular structure in a many-celled magnetotactic prokaryorte, *Arch. Microbiol.*, *154*, 18-22, 1990.

Snowball, I. F. Magnetic hysteresis properties of greigite ($Fe_3S_4$) and a new occurrence in holocene sediments for Swedish Lappland. *Phys. Earth Planet. Inter.*, *68*, 32-40, 1991.

Snowball, I. and Thompson, R. The occurrence of greigite in sediments from Loch Lomond, *J. Quaternary Sci. 3*, 121-125, 1988.

Snowball, I.F. and R. Thompson, A mineral magnetic study of holocence sedimentation in Lough Catherine, Northern Ireland. *Boreas 19*, 127-146, 1990.

Spender, M. R., J.M.D. Coey, and A.H. Morrish, The magnetic properties and Mössbauer spectra of synthetic samples of $Fe_3S_4$, *Can. J. Phys.*, *50*, 2313-2326, 1972.

Tric, E., C. Laj, C. Jehanno, J.P. Valet, and C. Kissel, High-resolution record of the upper Olduvai transition from Po valey Italy-sediments support for dipolar transition geometry, *Phys. EarthPlan. Interiors*, *65*, 319-336, 1991.

Uda, M., Synthesis of magnetic $Fe_3S_4$, *Sci. Pap. Inst. Phys. Chem. Res., Tokyo*, *62*, 14-23, 1968.

Worm, H.-U, P. J. Ryan, and S. K. Banerjee, Domain size, closure domain, and the importance of magnetorestriction in magnetite, *Earth Planet. Sci. Lett.*, *102*, 71-78, 1991.

Wyn, W., and D. J. Dunlop, Three-dimansional micromagnetic modelling of ferromagnetic domain structure, *Nature*, *337*, 634-637, 1989.


J. C. Diaz Ricci and J. L. Kirschvink, Division of Geological and Planetary Sciences, California Institute of Technology, Pasadena, CA 91125.

(Received August 15, 1991;
revised March 20, 1992;
accepted April 10, 1992.)